



Martian paleolake outlet canyons - Evidence for controls on valley network formation

Sharon J.M. Diamant^{a,*}, Rickbir S. Bahia^b, Elliot Sefton-Nash^b, Yamila Miguel^a

^a Leiden Observatory, Leiden University, Leiden, the Netherlands

^b European Space Research and Technology Centre, European Space Agency, Noordwijk, Netherlands

ARTICLE INFO

Keywords:

Mars
Martian valley networks
Martian paleolakes
Paleolake outlet canyons
Martian geomorphology

ABSTRACT

Martian valley networks (VNs) have been viewed as one of the most compelling pieces of evidence for ancient fluvial activity during the Late Noachian and Early Hesperian periods (3.7–3.5 Ga), likely as a result of precipitation (snowfall/rainfall). During this period, paleolakes also formed, predominantly due to water accumulation within impact crater interiors. Some of these paleolakes breached the rim of their basins (e.g., crater rim) which caused outburst flooding and incision of a paleolake outlet canyon over a short period of time (weeks to years). After the Late Hesperian, valley formation vastly decreased indicating a waning water cycle. There have been inferences that paleolake outlet canyons may have controlled the trajectories of adjacent valley networks that formed after them, yet no direct evidence has been observed. In this study, we map and apply paleohydrological, morphometric, and morphological calculations to two hydrological systems located west of the Tharsis Rise, where hydrological systems are defined as a combination of a paleolake outlet canyon and adjoining VNs. We aim to determine whether the paleolake outlet canyons show evidence of control on the trajectory of adjacent VNs and the impact this has on their development. We find that the paleolake outlet canyons do place control on the trajectories of adjacent VNs, causing them to detour from the regional slope direction and causing the basin to deviate from the natural fractal geometry formed by precipitation-fed fluvial incision. Additionally, the paleolake outlet canyons display a decrease in the cross-sectional area down their profile, indicating they experienced water loss as they were active. The examined paleolake outlet canyons have altered the evolution and interconnectivity of the adjoining VNs, leading to water loss, likely to the subsurface. Finally, given the proximity of these hydrological systems to the Tharsis Rise, we note that they display a complex history of fluvial and tectonic activity, indicating that fluvial activity both preceded and post-dates Tharsis-induced tectonic activity.

1. Introduction

The southern highlands of Mars are heavily incised by valley networks (VNs) (Fig. 1:A), which are evidence of an active hydrological cycle that is thought to have been at its peak during the Late Noachian – Early Hesperian (~3.7 Ga) (e.g., Carr, 1995; Carr and Chuang, 1997; Hynek et al., 2010; Bahia et al., 2022a). The incision of the VNs is mainly attributed to precipitation-fed (rainfall or snowfall) fluvial incision (e.g., Carr, 2012) which took place over tens to hundreds of thousands of years (Kleinbans et al., 2010; Hoke et al., 2011; Orofino et al., 2018). In addition to VNs, Mars is also home to paleolake outlet canyons (POCs) (e.g., Cabrol and Grin, 1999; Irwin III et al., 2005a; Fassett and Head III, 2008; Goudge et al., 2021). During the Late Noachian – Early Hesperian,

most paleolakes formed as the result of water accumulation within impact craters (Cabrol and Grin, 1999; Irwin III et al., 2005a; Fassett and Head III, 2008). Over 200 of these paleolakes were filled with a sufficient quantity of water to breach their rims, resulting in outburst flooding and incision of POCs (Goudge et al., 2018). Unlike valley networks, these POCs likely formed over very short time periods (weeks to years) (Irwin et al., 2002; Irwin et al., 2004a; Irwin and Grant, 2009; Goudge et al., 2018). Surfaces younger than the Early Hesperian display a substantial decrease in VNs and POCs, indicating that fluvial activity rapidly decreased after this era (Hynek et al., 2010; Bahia et al., 2022a), consistent with a waning Martian water cycle. This coincides with the loss of the Martian atmosphere as a result of large impacts and solar wind interactions (Andrews-Hanna and Lewis, 2011).

* Corresponding author.

E-mail address: s.diamant@4gems.nl (S.J.M. Diamant).

<https://doi.org/10.1016/j.icarus.2023.115835>

Received 11 June 2023; Received in revised form 22 September 2023; Accepted 3 October 2023

Available online 5 October 2023

0019-1035/© 2023 The Authors. Published by Elsevier Inc. This is an open access article under the CC BY license (<http://creativecommons.org/licenses/by/4.0/>).

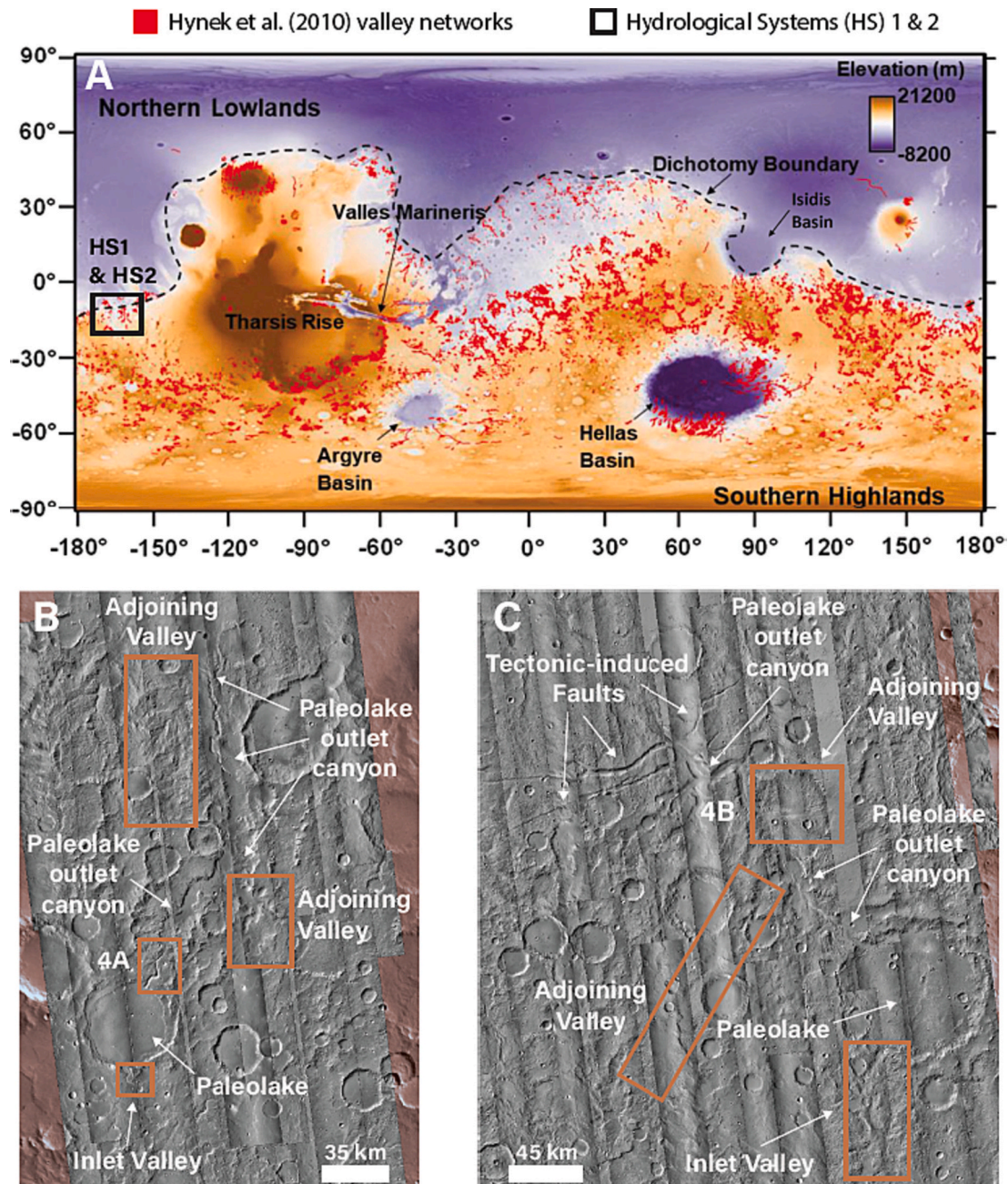


Fig. 1. (A) Topographic map of Mars showing the locations of major surface features dissected by valley networks (red lines – Hynek et al., 2010), with the locations of the two hydrological systems, HS1 and HS2, that we examine in this study (shown in panels B and C, respectively). (B) and (C) highlight the main features of the hydrological systems using the Context Camera image mosaic (CTX - ~ 6 m per pixel) overlain on the High-Resolution Stereo Camera (HRSC - ~ 50 – 100 m per pixel) images for the missing regions and the Mars Viking Colorized Global Mosaic basemap (orange layers, 461 m per pixel) (Smith et al., 1999). For VN1: Latitudinal extents = -11 to -15.8 ; Longitudinal extents = -172.8 to -175.3 (Forsythe and Zimbleman, 1995; Ori et al., 2000; Davis et al., 2022). For VN2: Latitudinal extents = -6.1 to -12.1 ; Longitudinal extents = -164.9 to -170.3 . North is up. (For interpretation of the references to colour in this figure legend, the reader is referred to the web version of this article.)

Recent analysis has revealed that POCs played a major role in the fluvial erosion of Mars' surface; although they only represent $\sim 3\%$ of the total length of VNs, they were responsible for 24% of the volume of eroded material (Goudge et al., 2021). That POCs caused plentiful erosion indicates that they were incised by substantial floods. The momentum of water in such substantial floods enabled flow directions to deviate from local slope directions. Yet, floods were too short-lived to erosionally "smooth out" valley profiles (Goudge et al., 2021). As a result, POCs display large undulations in their profile and do not follow the topographic slope direction, as evidenced by the observation that only 21% of POCs between 20°E – 20°W have orientations that conform

to surface slope direction (Bahia et al., 2022a).

Due to their ability to modify topography, recent studies hypothesized that POCs might have influenced the trajectories of VNs that formed after them (Goudge et al., 2021; Bahia et al., 2022a). If true, this has important implications for Mars' water cycle, because modified trajectories would impact the spatial distribution and magnitude of surface water fluxes. Valley networks created through water erosion, such as river valleys, typically widen and deepen downstream due to increased water volume and energy resulting from the confluence of tributaries (Knighton, 1998). This relationship can be complicated by changes in lithology (Craddock and Lorenz, 2017) leading to more/less

resistant bedrock, and fluid velocity (due to increases/reductions in slope) leading to increases/reductions in the erosional capacity of the river (Whipple and Tucker, 1999). Furthermore, water loss resulting from transmission losses and evaporation can significantly alter the dimensions of valleys and downstream channels, especially for systems fed by episodic flood events where water often overflows the channel banks and is therefore not fed down the main channel (Lange, 2005). Although most Martian VNs appear to follow the general relationship of increasing in size downstream, several networks display a decrease in valley cross-sectional area (Williams and Phillips, 2001). Detailed analysis of these valley networks may reveal the origin of these dimensional changes.

There has been no direct evidence that POCs are capable of altering adjoining VNs trajectories. In this study, we aim to investigate whether this is the case using, e.g., paleohydraulic equations, drainage analysis and observational evidence. If discovered, our second objective is to examine if the alteration of VNs trajectories might affect the water capacity of POCs down their profile. To proceed, we examine two hydrological systems, here defined as POCs with adjoining VNs, which are adjacent on the west side to the Tharsis Rise (Fig. 1), by calculating Hack's law exponent (Hack, 1957), discharge values (Irwin III et al., 2005b; Gou et al., 2019), and morphometric and morphological parameters (e.g., Williams and Phillips, 2001). Additionally, we find that the proximity of these hydrological systems to faults associated with Tharsis deformation reveals insight into the chronology between the formation of Tharsis and fluvial activity, the relative chronology of which is a matter of debate (e.g., Phillips et al., 2001; Bouley et al., 2016).

2. Hydrological systems analysis

2.1. Valley mapping

Two hydrological systems (POCs with adjoining VNs) were manually mapped in Context Camera images (CTX - ~6 m per pixel, Malin et al., 2007) overlain on the High-Resolution Stereo Camera (HRSC - ~50–100 +/- 6 m per pixel, Neukum and Jaumann, 2004) images for the missing regions and the Mars Viking Colorized Global Mosaic basemap (461 m per pixel, Smith et al., 1999) (Fig. 1:B and 1:C). This is done by following the identification criteria set out in previous valley mapping studies (e.g., Carr, 1995; Hynes et al., 2010; Bahia et al., 2022a, 2022c), i.e., “sublinear, incisional features, many of which form branching networks that slightly increase in size downstream and divide into smaller branches upslope.” (Bahia et al., 2022a). Moreover, the valleys and the POCs were also mapped in the inferred direction of flow (i.e., from source to termination). Furthermore, as stated in, e.g., Goudge et al., 2018, POCs were identified as troughs emerging as outlets from craters. In contrast to the sinuous form, troughs displaying linear, parallel or unconventional features are not considered to be fluvial tributaries as these features do not arise from a source of fluid uniformly distributed across the surface, such as precipitation. Further analysis is needed to determine the nature of these features.

2.2. Hack's law on precipitation-fed valley networks

Most Martian VNs that formed during the Late Noachian – Early Hesperian are hypothesized to have formed as a consequence of precipitation-fed fluvial incision (e.g., Craddock and Howard, 2002; Carr, 2012; Grau Galofre et al., 2020a, 2020b). It has long been established that there is an empirical relationship, referred to as Hack's law, between the main valley length and drainage area of precipitation-fed valley networks (Hack, 1957; Lou et al., 2023):

$$L = k_h A_D^n \quad (1)$$

where L is the length (m) of the valley measured along the principal stream from its source to any given point, A_D is the drainage area (m^2)

corresponding to that length of the stream, and k_h and n (the Hack's exponent) are constant. Analysis of all terrestrial precipitation-fed river basins has found that the value of n generally ranges between 0.5 and 0.6, with an average value of 0.54 ± 0.01 , revealing self-similarity as terrestrial river landforms are statistically identical, therefore, the value of n is independent of lithology and rainfall amounts (Mueller, 1973; Montgomery and Dietrich, 1992; Sassolas-Serrayet et al., 2018; Oliveira et al., 2019). Values of n outside of this range are rare. Values >0.6 are generally attributed to basins with small A_D ($< 100 km^2$) or those that have experienced topographic change that is not matched by sufficient fluvial incision (Hack, 1957; Willemin, 2000; Luo and Stepinski, 2012; Oliveira et al., 2019). Values of ~ 0.4 are attributed to basins with large drainage areas ($>$ several million km^2) (Mueller, 1973). Hack's Law is not only applicable to the main valley of the entire basin but can be applied at any point along any valley inside a sub-basin because of the fractal nature of drainage networks (Supplementary Fig. 1) (Rigon et al., 1996). Precipitation-fed Martian and Titan VNs have been found to follow Hack's Law and have n values $\simeq 0.5$ – 0.6 (Dhingra et al., 2018; Bahia et al., 2019, 2022b). This value can be compromised if the VN has experienced topographic modification after its termination or if it was not formed via a source of fluid uniformly distributed across its basin (e.g., groundwater sapping, ice-melt, subglacial incision and/or lava incision) (Bahia, 2022; Bahia et al., 2022b, 2022c). Hence, a valley network formed by uniform precipitation across the basin should (most likely) have an n value between 0.5 and 0.6 unless the basin has been caused to deviate from its natural fractal geometry. By applying Hack's Law to POC adjacent VNs, we can gain an insight into the source of fluid that formed them.

To conduct Hack's Law analysis on the POC adjacent VNs, we perform drainage network analysis to extract drainage area (A_D) values and surface flow directions. Drainage network analysis was performed on all POC adjacent VNs using a combination of the high-resolution stereo camera (HRSC - ~50–100 m per pixel, Neukum and Jaumann, 2004) digital elevation models (DEMs - POC 1: H2128_0000, H2117_0000 and H9324_0000; POC 2: H3207_0000, H2062_0000 and H3185_0000). This was done using the ArcMap 10.2.1 Spatial Analyst Toolset, following a technique called drainage network analysis that has previously been applied to Mars (e.g., Bahia, 2022; Fawdon et al., 2022). The valley networks are computationally generated using a “filled” version of the DEM using a three-step procedure established for terrestrial basins (Tarboton et al., 1989): (1) Following the standard practice in hydrological analysis (e.g., O'Callaghan and Mark, 1984), a fill function was applied to the DEMs to remove unwanted error and noise in the DEM. This process also fills sinks and basins making them drainable, however, craters on the outskirts of the drainage basin, with walls that would not allow the interior to drain outwards, do not add to the drainage area of the basin. Hence, the “real drainage” is likely to be fairly well represented by this process, and this process has been proven to be an effective method of delineating the drainage areas of Martian valley networks (e.g., Som et al., 2009; Penido et al., 2013; Fawdon et al., 2022; Bahia, 2022). This modified DEM is the ‘FILL’. When using the “FILL” tool, the selection of an appropriate z-value threshold, representing the depth to which depressions or sinks within a DEM are filled, is critical. This choice prevents the inadvertent removal of authentic sinks while effectively addressing only spurious ones, often attributed to inaccuracies in the DEM data. The specific depth of pit-filling required varies depending on the DEM dataset and its geographical location.

Unlike the surface of Earth, where flooded pits are generally data anomalies, the Martian surface is pitted with craters. The procedure removes the topographical information within, converting these craters into ‘lakes’. These craters only add to the drainage area of the network if they are dissected by the valley or have locations along their rims that would cause the interior to drain outwards. (2) Each site in the FILL is assigned a drainage pointer to the adjoining site that corresponds to the direction of the steepest slope. Using these drainage directions, the total

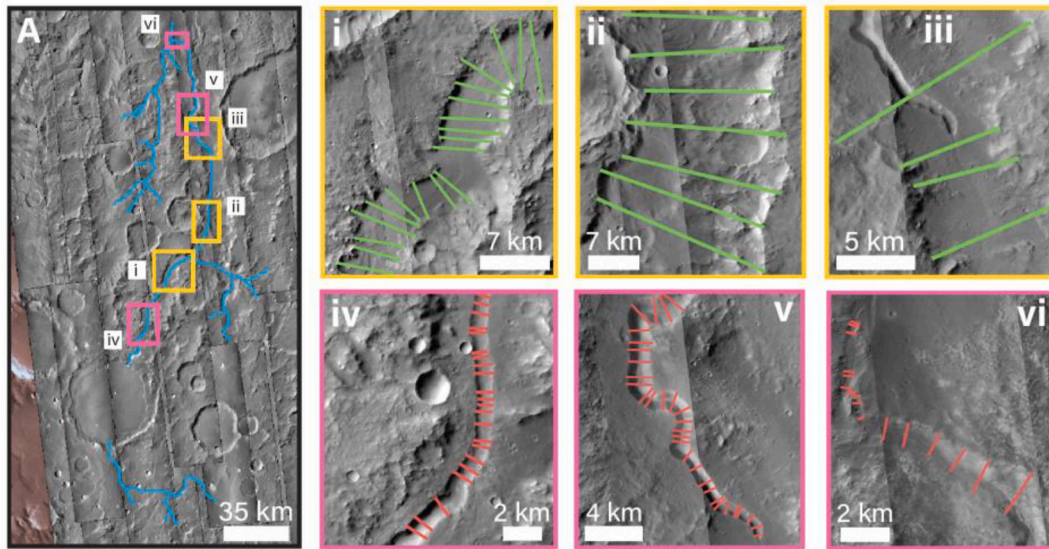


Fig. 2. Example of width measurements taken for the POC valley (green lines – i to iii) and inner channels (maroon lines – iv to vi) for hydrological system 1 (A). The blue lines represent the valley networks mapped by Hynek et al. (2010). (For interpretation of the references to colour in this figure legend, the reader is referred to the web version of this article.)

drainage area (A_D) is calculated for each site in the FILL. This A_D is the overall area of pixel coverage draining into any given site. (3) The valley network is manually delineated as the assemblage of sites at which $A_D \geq A_{ch}$. For terrestrial hydrology, A_{ch} denotes the minimum area of flow that causes channelization (Tarboton et al., 1991). A_{ch} is not known for Mars, so we delineated the valley network as pixels of flow convergence in the drainage map that correspond most closely with those visible in CTX images (e.g., Supplementary Fig. 8). Subsequently, the Hack's law exponent was determined for each system by plotting a least square polynomial fit together with $\ln(L)$ against $\ln(A_D)$ from Eq. (1).

2.3. Variation in discharge and cross-sectional area down the POC profile

Valley networks (VNs) are generally formed by rivers that form inner channels. The inner channel is the trough in which the river flows, and over time this channel erodes laterally and vertically causing a valley to form. VNs with inner channels are extremely rare on Mars, likely as a result of billions of years of erosion and aeolian infilling (e.g., Irwin III et al., 2005b). Considering POCs form due to outburst flooding, their 'channel' (i.e., the trough that accommodates the flowing fluid that formed it) is in fact the canyon valley itself. However, in our study, the POCs of interest have clearly defined inner channels within them (Fig. 2). By measuring the width at varying locations along the POCs and inner channels, as shown in Fig. 2, we can determine how discharge varied down their profiles. The discharge (m^3s^{-1}), Q , of the inner channel and valley is given by.

$$Q_{channel} = 1.9W_{channel}^{1.22} \quad (2)$$

$$Q_{valley} = 0.08W_{valley}^{1.908} \quad (3)$$

where W is the width of the inner channel ($W_{channel}$) and of the canyon valley (W_{valley}), respectively. Utilising discharge calculations, we can gain insight into the quantities of water that flowed through the inner channels (Irwin III et al., 2005b) and the valleys of the POCs (Gou et al., 2019), as stated in Eqs. (2) and (3) respectively. These discharge equations are based on empirical relationships on Earth (Irwin et al., 2005b; Gou et al., 2019). In turn, this provides information about the formation mechanisms of the inner channels and POCs, and indicates whether they were formed by the same or separate flow events. Considering discharge only accounts for the quantity of water flowing over a volume per

second, to determine the flow capacity of the POCs we also did a cross-sectional analysis of the POC profiles. This will assess whether POCs display evidence of water loss as they were active by analysing the alteration in their volume.

To determine the variation in discharge (Q) down the POCs, ~ 225 width measurements were manually taken, using CTX images, down each POC and inner channels (Fig. 2). The locations were systematically chosen by taking upstream, midstream and downstream measurements. Width measurements were only taken where one could confidently identify the valley and inner channel walls; however, we note that this is a somewhat subjective process (Bahia and Jones, 2020). Furthermore, the inner channels were not present throughout the whole POC profiles. Due to this, most of the time, the width measurements of both the inner channels and POCs could not have been taken at the same location. Moreover, the spacing length between the locations is uneven. Comparisons between the Q_{valley} and $Q_{channel}$ will aid in determining whether the POCs and inner channels had differing formation events. In a terrestrial context, it has been determined that, given a sufficient time for the channel to respond, inner channels that form VNs have an inverse relationship between channel slope (S) and width (W) (e.g., Finnegan et al., 2005; Yanites, 2018). To determine whether the POCs and the inner channels follow this relationship, we calculate S , using the HRSC DEMs, at locations where width measurements were taken. The slope of the identified valleys was quantified by extracting individual MOLA data points, down the centre of the valleys, each of which is characterized by specific latitude, longitude, and elevation values. To ensure uniformity in measurements, points were sampled at approximately 500-m intervals, and the contemporary slope was computed between consecutive point pairs utilising trigonometric principles. In cases where MOLA data points were spaced >500 m apart, the nearest neighbouring point along the valley profile was employed for calculations. Subsequently, the values of S are compared with $W_{channel}$ and W_{valley} .

The HRSC DEMs were also used to produce cross-sections at selected points along the POCs to determine how the cross-sectional area varies down their profiles. On both Earth and Mars, valleys generally increase in size down their profile with the introduction of additional tributaries, and therefore water volume (e.g., Marra et al., 2015). This may not be the case for subglacial VNs (e.g., Gran et al., 2013). Considering that POCs are the troughs that contain the water that is released by flood events: if the cross-sectional area of the POC decreases, it may indicate a decrease in discharge, therefore, leading to water loss.

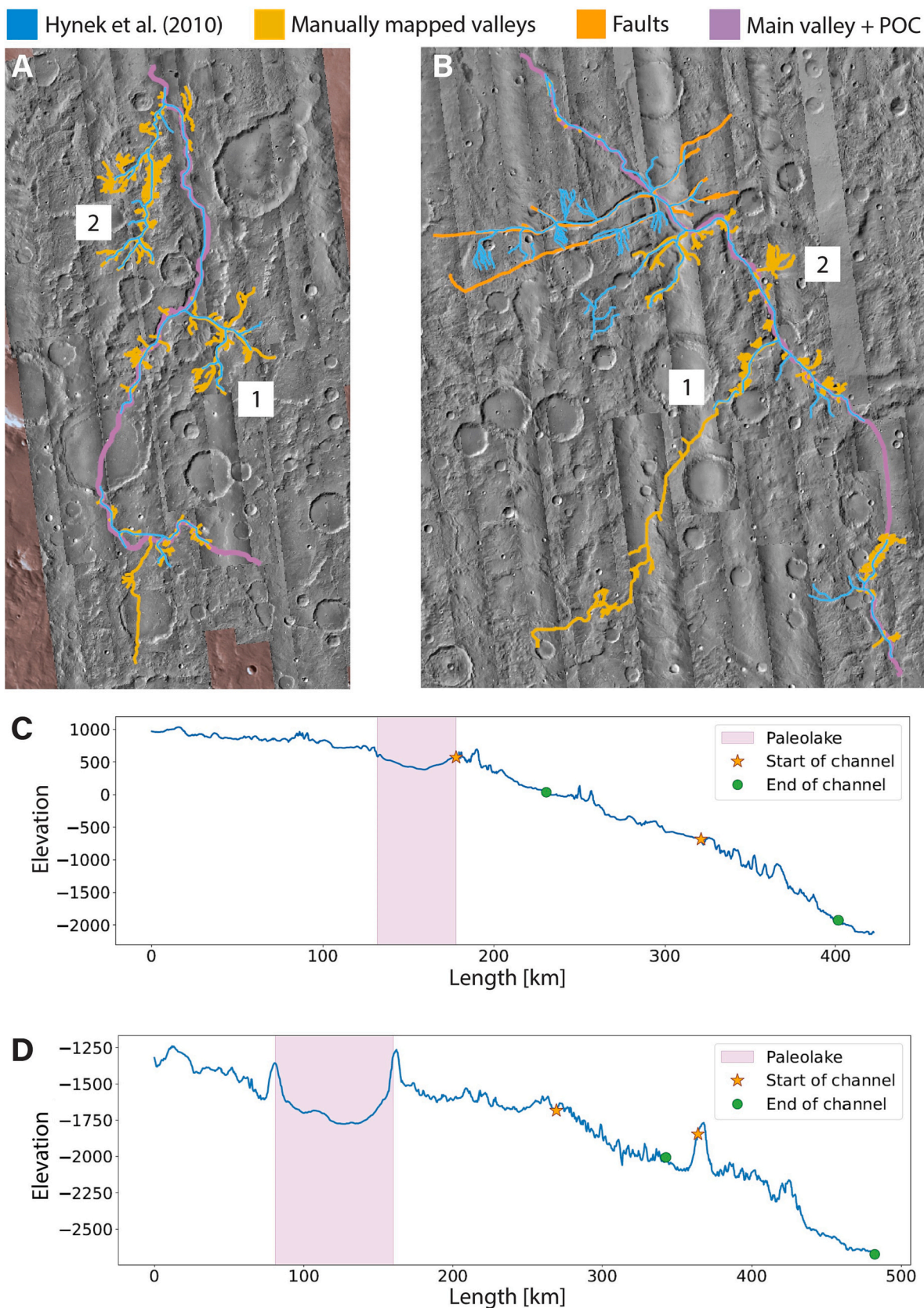


Fig. 3. Comparison between mapped valleys in this study (in yellow) and those mapped by Hynek et al. (2010 – in blue) for both hydrological system 1 (A) and 2 (B). Moreover, tectonic-induced faults (orange) were observed in hydrological system 2. (C) and (D) display the elevation profiles with start and end points of inner channels of hydrological system 1's POC and hydrological system 2's POC, respectively. Furthermore, (D) displays a large spike in the profile around 370 km which corresponds to the location of the tectonic-induced faults. The numbers in (A) and (B) refer to the number of the VNs for that system. (For interpretation of the references to colour in this figure legend, the reader is referred to the web version of this article.)

Table 1

Summary of all measured and calculated values for both hydrological systems (POCs with adjoining VNs). n is the Hack's law exponent for a given valley network. The length of the POCs and VNs was determined by manually mapping polylines in ArcGIS using CTX and HRSC data. In turn, the total drainage area is a result of drainage area analysis using HRSC DEMs. Using extracted individual MOLA data points, the slope was computed between consecutive point pairs utilising the trigonometric principle. Hack's exponent and the average discharge (including the whole range of discharge) were determined by Eq. (1) using a power law fit and, Eqs. (2) and (3), respectively.

Hydrological system	Total length to the nearest km (km)	Total Drainage Area (m ²)	Slope (m/m)	n	Average (and range) discharge (m ³ /s)
1 POC	244	–	0.011	–	4.24×10^6 (7.77×10^5 to 1.59×10^7)
VN 1	71	1.59×10^9	0.022	0.46 ± 0.06	–
VN 2	157	4.01×10^9	0.019	0.74 ± 0.08	–
2 POC	322	–	0.0042	–	2.71×10^6 (9.93×10^4 to 2.18×10^7)
VN 1	260	17.54×10^9	0.0055	0.57 ± 0.06	–
VN 2	90	1.69×10^9	0.010	0.61 ± 0.16	–

3. Results and observations

Mapping of the two hydrological systems using CTX and HRSC images revealed that both POCs have adjoining VNs, resulting in an increase of ~900% in valley length compared to the previous valley map (Hynek et al., 2010) (Fig. 3:A and 3:B). All measured and calculated results are summarised in Table 1.

3.1. Drainage network analysis – evidence of POC control on VN development

To understand the formation mechanism of the two hydrological systems, we have performed a drainage network analysis of the VNs adjacent to the POCs in both systems. The analysis reveals that, for the POC-adjacent VNs, VNs are present with n values between 0.5 and 0.6 (Fig. 4) indicative of formation via a source of fluid uniformly distributed across the basin (e.g., precipitation). POC 1:VN 2 (i.e., VN2 adjacent to POC1) (Fig. 4) has an n value outside of this range; however, the first ~70 km of the network has an n of ~0.6, after which point the valley appears to have a trajectory towards the POC, with the final reaches of the VN having trajectory away from the predicted flow paths based on local topography. This may indicate that as the river that formed POC 1:VN 2 came closer to the POC's trough it was diverted from the trajectory defined by the surface slope. This is similar to POC 2:VN 2 and POC 2:VN 1 (Fig. 4), which have an n value within this range, but it is apparent the correlation between L and A becomes compromised as the valley reaches the POC (Fig. 4), indicating its basinal shape has been dictated by the POC.

Hack's law analysis could not be applied to the two inlet valleys, i.e., tributaries that flow into the paleolake basin. Comparison between the predicted flow paths generated from the DEM and those observed in imagery reveals large differences (Supplementary Fig. 5). This may indicate that the inlet areas have been heavily altered since the emplacement of the inlet VN, or the source of fluid that formed the VN

was not uniformly distributed across the basin - e.g., localised precipitation or, as predicted for other inlet valleys on Mars (Bamber et al., 2022), drainage head erosion fed by groundwater sapping or subglacial incision.

Furthermore, Hack's law was not employed to four troughs in hydrological system 2. Satellite imagery observations show that the troughs are linear and parallel in shape, as opposed to the sinuous form of traditional valley networks (Supplementary Fig. 7:A). Additionally, the elevation profiles of these troughs reveal a high variety in elevation suggesting a low probability of an active fluvial valley as it favours downward elevation (Supplementary Fig. 7:B). Consequently, we interpret these troughs to be tectonic-induced faults. This is feasible as, next to the previous reasonings, the hydrological systems' location is close to Tharsis Rise.

3.2. Discharge and cross-sectional analysis of the POCs and their inner channels

To further examine the effects on the alteration of both the POCs and adjoining VNs topography, we applied discharge and cross-sectional analysis to assess the water capacity of POCs (and inner channels included) down their profile. Discharge analysis reveals orders of magnitude difference between the internal channels and POCs (Fig. 5). We note that the inner channels are not present throughout the whole POC, hence there are gaps in the discharge measurements down the profile (Fig. 5). Average discharge values of POCs range from 0.24×10^7 to 0.4×10^7 m³/s while those of inner channels be amongst 0.36×10^4 to 1.1×10^4 m³/s.

Unlike most VNs, which display a general increase in discharge (and width, shown in Supplementary Fig. 2) down their profile, in terms of discharge, the inner channels display a general decrease, and POCs display little change (Fig. 5). Although width changes may be attributed to variations in slope, we observe no systematic relationship between the two (Supplementary Fig. 3). Additionally, the cross-sectional analysis reveals a general decrease in POC dimensions down profile, indicating a loss in fluid flow (Supplementary Fig. 4). However, the width: depth ratio remains fairly consistent (~20), as the POC is decreasing in both dimensions down its profile, comparable to the general population of fluvially formed Martian valleys (Williams and Phillips, 2001). Moreover, comparing the inner channel width and valley width along the POCs, the average ratio of inner channel width to valley width is 0.1 ± 0.03 (VS1) and 0.088 ± 0.03 (VS2), which is lower than the ratio of 0.14 ± 0.03 reported by Penido et al. (2013) for Martian VNs that appear to be fed by precipitation. This suggests that the inner channels and/or POCs didn't form by precipitation.

3.3. Geomorphological evidence of a complex fluvial and tectonic history

Additionally, the detailed valley mapping of these systems reveals a complex fluvial and tectonic history for this boundary region between the northern lowlands and southern highlands of Mars. Hydrological system 2 displays ancient hanging valleys (Fig. 7:A), which are highly degraded and appear to have been dissected by faults. The POC has clearly cut through these faults (Fig. 7:A). The walls of the POC have been incised by adjacent VNs, one of which converges forming a channel that is directed down the centre of the POC (Fig. 6:B).

Similar to hydrological system 2, hydrological system 1 displays evidence that the adjacent VNs likely formed, or at least were active, after the termination of the POCs (e.g., Fig. 7:C). Examining the elevation profile of the main valley of VN 1 (Fig. 7:B) reveals a notable, possible knickpoint, indicative of continued fluvial incision into the valley wall of the POC after its establishment.

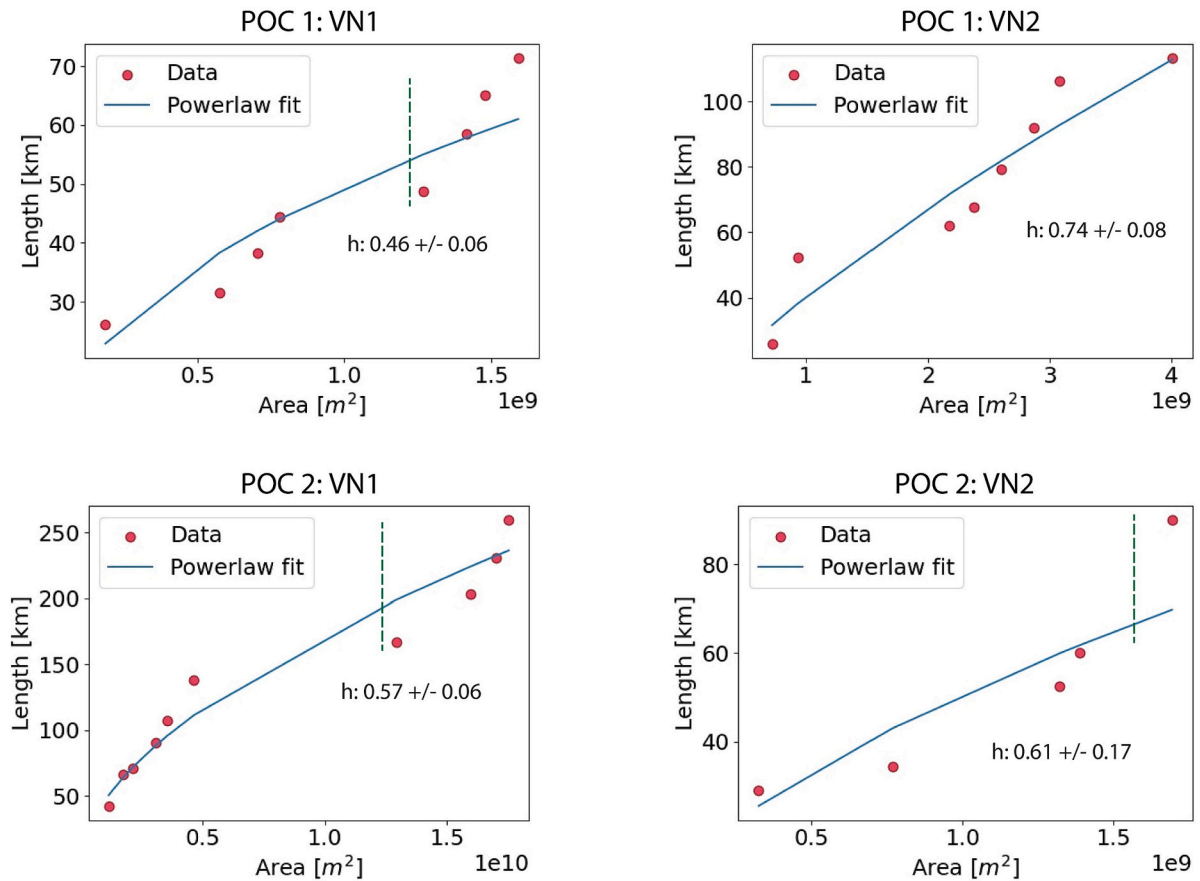


Fig. 4. Results of Hack's Law analysis applied to the main valleys of the adjoining VNs to the POCs. The green dashed lines indicate where the data deviates from the Hack's law fit. The h is the Hack's law exponent. (For interpretation of the references to colour in this figure legend, the reader is referred to the web version of this article.)

4. Discussion and implications

4.1. Paleolake outlet canyon controls on the trajectories and evolution of Martian valley networks

Examining two hydrological systems using paleohydraulic equations, discharge analysis and observational evidence, we have addressed whether POCs alter the adjacent-VNs trajectories that formed after them. If proven, we have assessed if the alteration of VNs trajectories might have influenced the water capacity of the POCs down their profile.

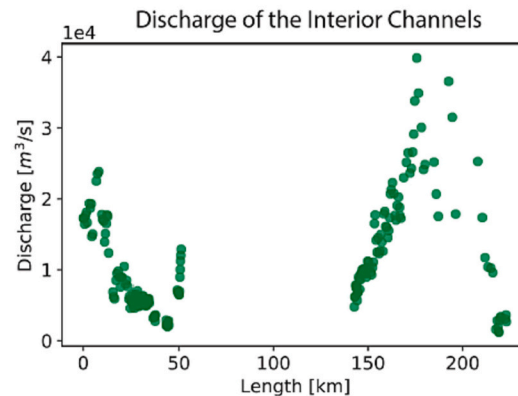
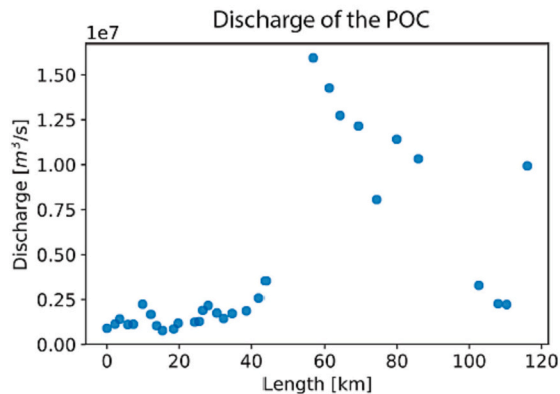
The examined POCs display hydrological and geomorphological evidence for control on the trajectories of subsequently formed adjacent VNs. Adjacent VNs appear to have been redirected away from the local slope direction and also on entry to the POC they have formed channels that are directed down the POC profile. The difference in the average ratio of channel width to valley width between the POCs (0.1 ± 0.03 for VS1, while 0.088 ± 0.03 for VS2) and precipitation-fed Martian VNs (0.14 ± 0.03) (Penido et al., 2013), may indicate that the inner channels and POCs have different origins, but more work is needed to assert this. Moreover, as the discharge is proportional to the width, discharge measurements result in orders of magnitude differences between the inner channels and POCs (Fig. 5). The discharges of the POCs ($0.24 \times 10^7 - 0.4 \times 10^7 \text{ m}^3/\text{s}$) are much larger than those of the inner channels ($0.36 \times 10^4 - 1.1 \times 10^4 \text{ m}^3/\text{s}$), with values more consistent with a terrestrial explosive outburst flood event (O'Connor and Baker, 1992; Gupta et al., 2007), i.e., those associated with POC formation (e.g., Irwin et al., 2002, 2004a; Goudge et al., 2016, 2021). The discharge of the inner channels is comparable to that of other inner channels on Mars interpreted to have formed via precipitation (Jaumann et al., 2005;

Irwin et al., 2004b; Irwin III et al., 2005b). This aligns with the geomorphological evidence, especially for hydrological system 2 where the channel can be observed emerging from an adjacent VN (Fig. 6:B). For hydrological system 1, the channel emerges from the paleolake. The significant channel width to valley width ratio and discharge difference between the inner channels and POCs suggests that the inner channels were likely formed by later fluvial activity, which could have been continued, potentially precipitation-fed fluvial incision.

Additionally, we have examined the length-elevation profiles of the POCs and adjoining VNs to gain more insight into the variation of the geometry down their profile. POCs have large elevation undulations in their longitudinal profiles (Fig. 3:C and 3:D). Fig. 3:D, around 370 km, displays a large spike in the profile which corresponds to the location of the tectonic-induced faults. Such undulations are not present within the VNs (other than knickpoints) and are uncommon for VNs formed via precipitation (Grau Galofre et al., 2020b). Given that the rivers responsible for VNs were directed into the POCs, occupying the POCs predefined troughs, the VNs would have encountered topographic highs and valley walls (Fig. 3). This redirection likely hindered their lateral migration and defined their trajectory, an effect absent without this influence.

Cross-sectional and discharge analysis of the POCs indicates that they experienced water loss down their profiles whilst active. Given that these POCs formed over short periods (weeks to years) (Irwin et al., 2002; Irwin et al., 2004a; Irwin and Grant, 2009; Goudge et al., 2018), during climatic conditions where liquid water was likely stable at the surface, water loss due to evaporation was likely limited (e.g., Ramirez et al., 2020). It is possible that the large undulations in the POC profile led to residual fluid pooling and water loss due to subsurface drainage

A Hydrological System 1 - Discharge



B Hydrological System 2 - Discharge

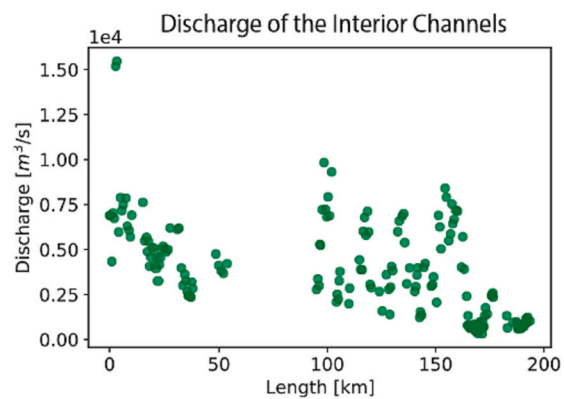
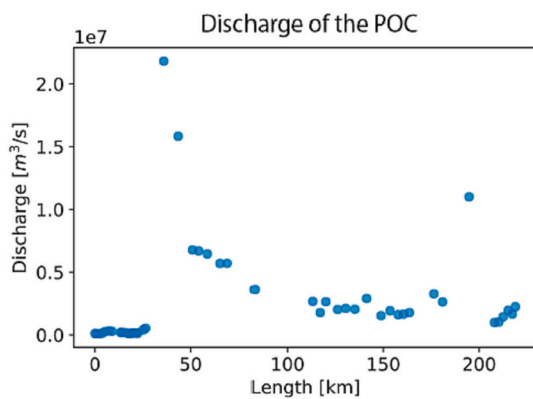


Fig. 5. Results of discharge vs. length down POC and inner channel for both hydrological systems; (a) is the result for hydrological system 1, and (b) for hydrological system 2. In both cases there is a notable difference in the discharge values for the POCs and the inner channels.

and increased evaporation. Unlike the POC floods, the likely precipitation-fed rivers that flowed from adjacent VNs into the POCs would have been incapable of overcoming the topographic highs of the POCs profile, likely leading to pooling and subsurface drainage. This may also explain the appearance and disappearance of inner channels in the POCs, whose locations appear to somewhat correlate with topographic highs in the profile (Fig. 3:C and 3:D).

An alternative to fluid loss is a change in slope, decrease in erodibility, reduction of flood power or carrying capacity due to changes in velocity and/or bed friction. However, this has to account for the decreases in the valley cross-sectional area of HS1 ($2.86 \times 10^7 \text{ m}^2$) and HS2 ($1.02 \times 10^6 \text{ m}^2$). Based on Supplementary Fig. 9, we can deduce that change in slope is not the major factor contributing to valley cross-sectional area changes. Given these huge differences in cross-sectional area, we favour the hypothesis of water loss.

These valley systems display evidence that the POCs have controlled the trajectories of adjacent VNs. In doing so, they not only altered the distribution of surface water inventories by removing water from paleolakes, but also by altering the interconnectivity of VNs by causing their orientation to not conform to the direction of the local slope. This may have led to excess water loss to the subsurface by causing the rivers to be funnelled down profiles with topographic impassable obstacles within the POCs leading to pooling and enhanced infiltration.

4.2. The chronology between fluvial activity and Tharsis Rise tectonic deformation

Additionally, the hydrological systems we examine in this study are in close proximity to Tharsis Rise and show a diverse history of fluvial and tectonic activity, which holds implications for both the fluvial and topographic evolution of Mars. Hydrological system 2 appears to have the following chronology: (i) initial fluvial incision leading to the formation of the now degraded hanging valleys. These hanging valleys are heavily degraded and have undergone tectonic modification after their emplacing, which would likely result in unrepresentative values from morphological and hydrological analysis. However, the planforms of these systems are uncharacteristic of precipitation-fed or groundwater-fed sapping systems, and more like subglacial terrestrial systems, such as those observed in the Devon Islands (Grau Galofre et al., 2018; Grau Galofre et al., 2020b) (Supplementary Fig. 6). Hence, we speculate that they could be subglacial in origin, however, in the absence of further analysis, this cannot be certain. (ii) Tectonic activity led to the formation of two parallel faults, which dissect the hanging valleys. Given the location and orientation of these faults, they likely formed as a result of Tharsis-induced topographic modification (Bouley et al., 2018). (iii) inlet valley initiation and paleolake formation. Given that these inlet valleys do not follow Hack's law they may have formed via localised precipitation, groundwater sapping, or subglacial ice melt. (iv) Paleolake outburst flooding occurred, with discharge values reaching $\sim 2.0 \times 10^7 \text{ m}^3 \text{ s}^{-1}$, resulting in the POC, which, in turn, has incised the faults.

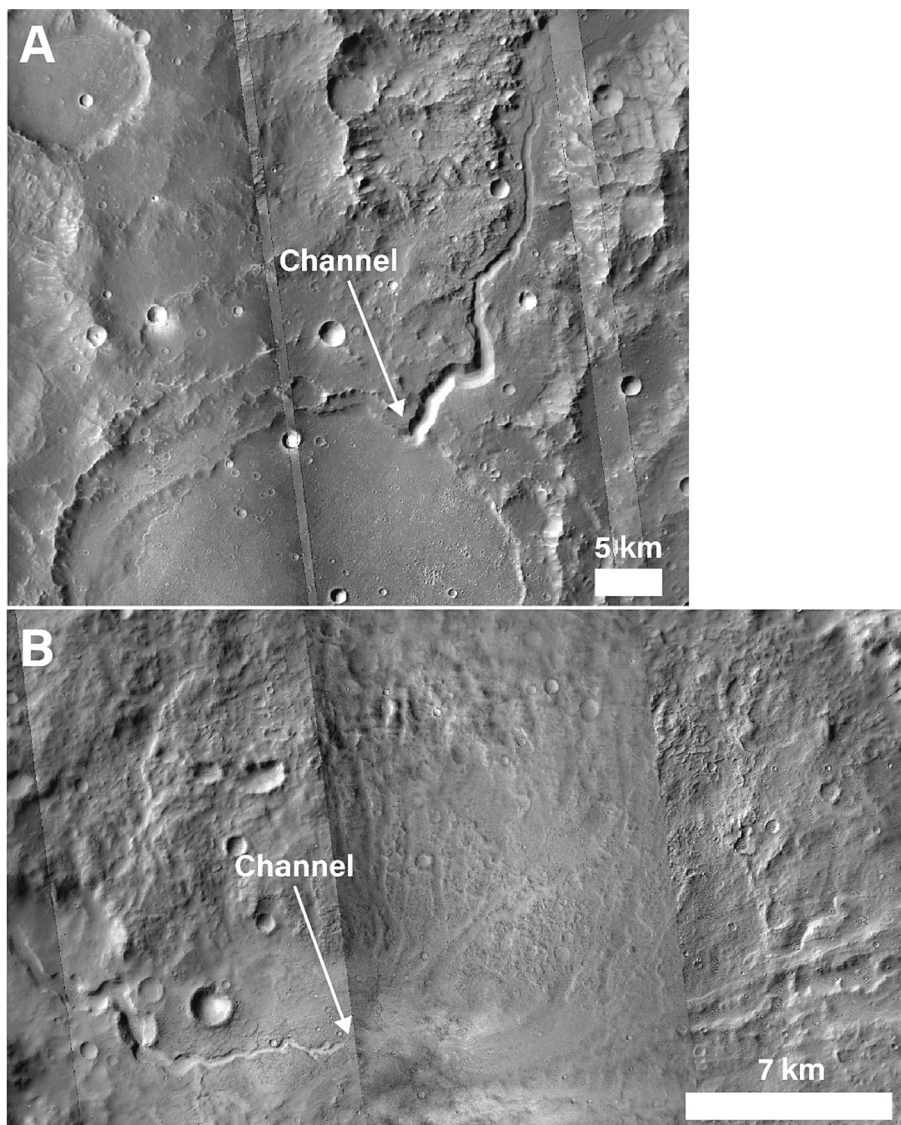


Fig. 6. Source of inner channels for (A) hydrological system 1 and (B) hydrological system 2. It is apparent that the inner channel for hydrological system 1 starts at the head of the POC, whereas for hydrological system 2 the inner channel emerges from an adjoining VN (VN 2 of hydrological system 2).

The outburst event was a result of the paleolake water levels being high enough to either overflow the rim or breach the rim's interior (e.g. dam burst). This indicates climatic conditions during this period were adequate for sustained and large quantities of liquid water at the surface, sufficient for filling and, possibly, breaching or overflowing of the paleolake, (v) After the formation of the POC, VN formation occurred, likely as the result of precipitation, resulting in the incision of the valley walls of the POC, evidenced by possible knickpoints, and central channel formation within the POC's main trough.

Hydrological system 1 likely had a similar formation chronology to hydrological system 2. However, the inlet valley and/or paleolake may have experienced reactivation, with a sufficient quantity of fluid to cause a channel to form within the POC. Additionally, we do not observe any potential subglacial channels in Hydrological system 1.

The chronology between the formation of the Tharsis Rise and valley networks is a matter of debate. Phillips et al. (2001) compared the orientation of large valleys and topographic slope direction associated with the development of the Tharsis Rise and concluded that their orientation was defined by Tharsis-induced slopes, indicating that valley development predominantly post-dates Tharsis. Conversely, Bouley et al. (2016) found that the orientations of VNs are consistent with

surface slope directions of the equilibrium shape of Mars with Tharsis removed, suggesting they predominantly pre-date it. Our study area displays a more complex history, with fluvial incision taking place prior to, potentially due to subglacial activity, and after tectonic activity induced by the Tharsis Rise, likely due to precipitation-fed activity.

5. Conclusion

In this study we use paleohydraulic equations and observational evidence to address two questions, the first one being: Did paleolake outlet canyons (POCs) control the trajectories of adjacent valley networks (VNs) that formed after them? If proven, does this control on VN trajectories have an impact on the water capacity of POCs down their profile? To proceed, we performed high-resolution mapping on two hydrological systems (a POC with adjoining VNs), located to the west of the Tharsis Rise. Using CTX images, we identified far more small valleys, indicating that higher-resolution mapping is required to produce a comprehensive map of Martian valleys., as previously highlighted by Bahia et al. (2022a). To understand the formation mechanism of the systems we then perform drainage network analysis (Hack, 1957) to the adjoining VNs and discharge calculations (Irwin III et al., 2005b; Gou

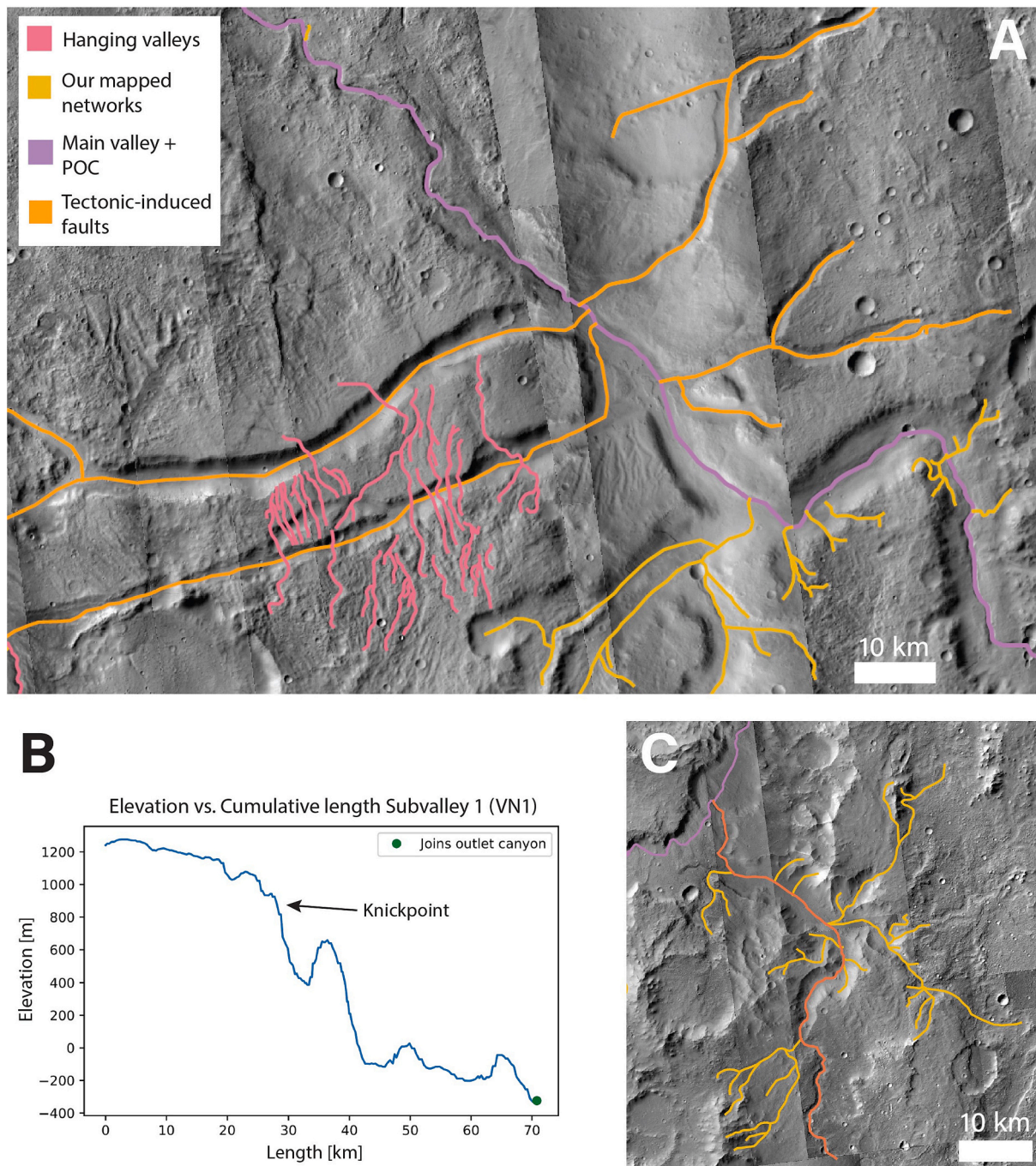


Fig. 7. (A) Zoomed in area of hydrological system 2, showing the presence of ancient hanging valleys (pink) that have been dissected by faults (orange). These faults have subsequently been dissected by the POC (purple). (B) Elevation profile of hydrological system 1's VN1 (C) first order valley as shown in orange, which displays a possible knickpoint. (For interpretation of the references to colour in this figure legend, the reader is referred to the web version of this article.)

et al., 2019) to the POCs and their inner channels. We also examine the length-elevation profiles of the POCs and adjoining VNs, and how the geometry of the POCs trough varies down its profile. Our analysis revealed that the POCs display large elevation undulation in their profiles, which indicates the flow that formed the POCs had velocities capable of overcoming these topographic highs. This is plausible given that they have discharge values of $\sim 2.0 \times 10^7 \text{ m}^3 \text{ s}^{-1}$. However, it appears that these undulations cause water to pool leading to water loss, as the cross-sectional areas of the POCs decrease down their profiles.

Our findings reveal that the adjoining VNs have trajectories and basins that have been defined by the POCs, resulting in orientations away from the surface slope direction when close to the POC. The rivers

that formed the VNs would have occupied these POCs, encountering the topographic undulations. As they encounter the topographic highs they will pool, resulting in water loss to the subsurface. This may explain the presence of channels that occupy the POCs, likely related to the rivers that originate from the adjacent VNs, which disappear as they encounter topographic highs and reappear at lower elevations. Additionally, the discharge values of the inner channels generally decrease down the POC profile. These POCs have altered the evolution and interconnectivity of the VNs, leading to water loss, likely to the subsurface.

Furthermore, we have investigated the relative chronology between the formation of valley networks and the Tharsis Rise. Our observations suggest that fluvial activity likely occurred prior to and after tectonic

activity associated with the formation of the Tharsis Rise. The origin of this fluvial activity may have varied through time, starting with a possible subglacial origin, more research is needed to confirm this, followed by a later precipitation-fed incision.

Declaration of Competing Interest

The authors declare that they have no known competing financial interests or personal relationships that could have appeared to influence the work reported in this paper.

Data availability

Data will be made available on request.

Acknowledgements

Sharon Diamant would like to acknowledge support from the Astronomy (MSc) from Leiden University, and the Leiden-ESTEC Masters Projects Programme. Rickbir S. Bahia would like to acknowledge support from an ESA Research Fellowship. Elliot Sefton-Nash is supported by the European Space Agency. Yamila Miguel would like to acknowledge support from Leiden University. Furthermore, we want to express our gratitude to Tim Goudge for the fruitful discussions and who made us aware of the knickpoints in our elevation profiles. Moreover, we would like to thank Zach Dickeson for giving us more insight on the capacities of paleolake outlet canyons. All research data supporting this publication are directly available from the USGS PILOT Website (<https://pilot.wr.usgs.gov>) and ESA's Planetary Data System (<https://psa.esa.int>). We would also like to thank the two reviewers, and editor, for taking the time to review this manuscript and provide helpful comments.

Appendix A. Supplementary data

Supplementary data to this article can be found online at <https://doi.org/10.1016/j.icarus.2023.115835>.

References

- Andrews-Hanna, J.C., Lewis, K.W., 2011. Early Mars hydrology: 2. Hydrological evolution in the Noachian and Hesperian epochs. *J. Geophys. Res. Planets* 116. <https://doi.org/10.1029/2010JE003709> e200207.
- Bahia, R.S., 2022. Morphological and hydrological analysis of volcanic flank valleys – evidence for a volcanic origin. *Planet. Space Sci.* 223, 105592. <https://doi.org/10.1016/j.pss.2022.105592>.
- Bahia, R.S., Jones, M., 2020. The subjectivity in identification of Martian channel networks and its implication for citizen science projects. *Earth Moon Planet.* 123 (3–4), 45–59. <https://doi.org/10.1007/s11038-020-09530-y>.
- Bahia, R.S., Jones, M., Covey-Crump, S., Mitchell, N., 2019. The Application of Hack's Law and Flint's Law to Mars and its Implications for the Noachian Climate. 50th LPSC, p. 1197.
- Bahia, R.S., Covey-Crump, S., Jones, M.A., Mitchell, N., 2022a. Discordance analysis on a high-resolution valley network map of Mars: assessing the effects of scale on the conformity of valley orientation and surface slope direction. *Icarus* 383, 115041. <https://doi.org/10.1016/j.icarus.2022.115041>.
- Bahia, R.S., Covey-Crump, S., Jones, M., Mitchell, N., 2022b. The application of Hack's law and Flint's law to Martian valley networks and its implications for the Noachian climate. *Icarus*. In Preparation.
- Bahia, R.S., Grau Galofre, A., Mitchell, N., Covey-Crump, S., Jones, M., 2022c. The fluvial and glacial history of the Argyre region - as revealed by new valley mapping techniques. *Icarus*. Under Review.
- Bamber, E.R., Goudge, T.A., Fassett, C.I., Osinski, G.R., 2022. Constraining the formation of paleolake inlet valleys across crater rims. *Icarus* 378, 114945. <https://doi.org/10.1016/j.icarus.2022.114945>.
- Bouley, S., Baratoux, D., Matsuyama, I., Forget, F., Séjourné, A., Turet, M., Costard, F., 2016. Late Tharsis formation and implications for early Mars. *Nature* 531, 344–347. <https://doi.org/10.1038/nature17171>.
- Bouley, S., Baratoux, D., Paulien, N., Missenard, Y., Saint-Bézar, B., 2018. The revised tectonic history of Tharsis. *Earth Planet. Sci. Lett.* 488, 126–133. <https://doi.org/10.1016/j.epsl.2018.02.019>.
- Cabrol, N.A., Grin, E.A., 1999. Distribution, classification, and ages of Martian impact crater lakes. *Icarus* 142, 160–172. <https://doi.org/10.1006/icar.1999.6191>.

- Carr, M.H., 1995. The Martian drainage system and the origin of valley networks and fretted channels. *J. Geophys. Res.* 100 (E4), 7479. <https://doi.org/10.1029/95je00260>.
- Carr, M.H., 2012. The fluvial history of Mars. *Phil. Trans. R. Soc. A* 370, 2193–2212. <https://doi.org/10.1098/rsta.2011.0500>.
- Carr, M.H., Chuang, F.C., 1997. Martian drainage densities. *J. Geophys. Res. Planets* 102 (E4), 9145–9152. <https://doi.org/10.1029/97JE00113>.
- Craddock, R.A., Howard, A.D., 2002. The case for rainfall on a warm, wet early Mars. *J. Geophys. Res.* 107, 1–31. <https://doi.org/10.1029/2001JE001505>.
- Craddock, R.A., Lorenz, R., 2017. The changing nature of rainfall during the early history of Mars. *Icarus* 293, 172–179. <https://doi.org/10.1016/j.icarus.2017.04.013>.
- Davis, J.M., Aranos, L., Dickeson, Z.I., Fawdon, P., 2022. The evolution of ancient fluvial systems in Memnonia Sulci, Mars: impact crater damming, aggradation, and a large water body on the dichotomy? *J. Geophys. Res. Planets* 127 (2). <https://doi.org/10.1029/2021JE00702> e2021JE007021.
- Dhingra, R.D., Barnes, J.W., Yanites, B.J., Kirk, R.L., 2018. Large catchment area recharges Titan's Ontario lacus. *Icarus* 299, 331–338. <https://doi.org/10.1016/j.icarus.2017.08.009>.
- Fassett, C.I., Head III, J.W., 2008. The timing of Martian valley network activity: constraints from buffered crater counting. *Icarus* 195, 61–89. <https://doi.org/10.1016/j.icarus.2007.12.009>.
- Fawdon, P., Balme, M., Davis, J., Bridges, J., Gupta, S., Quantin-Nataf, C., 2022. Rivers and lakes in Western Arabia Terra: the fluvial catchment of the ExoMars 2022 rover landing site. *JGR Planets* 127. <https://doi.org/10.1029/2021JE007045> e2021JE007045.
- Finnegan, N.J., Roe, G., Montgomery, D.R., Hallet, B., 2005. Controls on the channel width of rivers: implications for modelling fluvial incision of bedrock. *Geology* 33 (3), 229–232. <https://doi.org/10.1130/G21171.1>.
- Forsythe, R.D., Zimbleman, J.R., 1995. A case for ancient evaporite basins on Mars. *J. Geophys. Res. Planet* 100 (E3), 5553–5563. <https://doi.org/10.1029/95JE00325>.
- Gou, S., Yue, Z., Di, K., Xu, Y., 2019. Comparative study between rivers in Tarim Basin in Northwest China and Evros Vallis on Mars. *Icarus* 328, 127–140. <https://doi.org/10.1016/j.icarus.2019.03.017>.
- Goudge, T.A., Fassett, C.I., Head, J.W., Mustard, J.F., Aureli, L.K., 2016. Insights into surface runoff on early Mars from paleolake basin morphology and stratigraphy. *Geology* 44 (6), 419–422. <https://doi.org/10.1130/G37734.1>.
- Goudge, T.A., Fassett, C.I., Mohrig, D., 2018. Incision of paleolake outlet canyons on Mars from overflow flooding. *Geology* 47, 7–10. <https://doi.org/10.1130/G45397.1>.
- Goudge, T.A., Morgan, A.M., Stucky de Quay, G., Fassett, C.I., 2021. The importance of lake breach floods for valley incision on early Mars. *Nature* 597, 645–649. <https://doi.org/10.1038/s41586-021-03860-1>.
- Gran, K.B., Finnegan, N., Johnson, A.L., Belmont, P., Wittkop, C., Rittenour, T., 2013. Landscape evolution, valley excavation, and terrace development following abrupt postglacial base-level fall. *GSA Bull.* 125, 1851–1864. <https://doi.org/10.1130/B30772.1>.
- Grau Galofre, A., Jellinek, A.M., Osinski, G.R., Zanetti, M., Kukko, A., 2018. Subglacial drainage patterns of Devon Island, Canada: detailed comparison of rivers and subglacial meltwater channels. *Cryosphere* 12, 1461–1478. <https://doi.org/10.5194/tc-12-1461-2018>.
- Grau Galofre, A., Bahia, R.S., Jellinek, A.M., Whipple, K.X., Gallo, R., 2020a. Did Martian valley networks substantially modify the landscape? *Earth Planet. Sci. Lett.* 547, 116482. <https://doi.org/10.1016/j.epsl.2020.116482>.
- Grau Galofre, A., Jellinek, A.M., Osinski, G.R., 2020b. Valley formation on early Mars by subglacial and fluvial erosion. *Nat. Geosci.* 13, 663–668. <https://doi.org/10.1038/s41561-020-0618-x>.
- Gupta, S., Collier, J.S., Palmer-Felgate, A., Potter, G., 2007. Catastrophic flooding origin of shelf hydrological systems in the English Channel. *Nature* 448, 342–345. <https://doi.org/10.1038/nature06018>.
- Hack, J.T., 1957. Studies of longitudinal stream profiles in Virginia and Maryland. In: U. S. Geol. Surv. Prof. Pap. 294-B, pp. 45–97. <https://doi.org/10.3133/pp294B>.
- Hoke, M.R.T., Hynek, B., Tucker, G.E., 2011. Formation timescales of large Martian valley networks. *Earth Planet. Sci. Lett.* 312, 1–12. <https://doi.org/10.1016/j.epsl.2011.09.053>.
- Hynek, B.M., Beach, M., Hoke, M.R.T., 2010. Updated global map of Martian valley networks and implications for climate and hydrologic processes. *J. Geophys. Res.* 115, 1–14. <https://doi.org/10.1029/2009JE003548>.
- Irwin, R.P., Grant, J.A., 2009. Megaflooding on Earth and Mars. Cambridge Univ. Press, pp. 209–224. <https://doi.org/10.1017/CBO9780511635632>.
- Irwin III, R.P., Howard, A.D., Craddock, R.A., Moore, J.M., 2005a. An intense terminal epoch of widespread fluvial activity on early Mars: 2. Increased runoff and paleolake development. *J. Geophys. Res. Planets* 110. <https://doi.org/10.1029/2005JE002460> e12S15.
- Irwin III, R.P., Craddock, R.A., Howard, A.D., 2005b. Interior channels in Martian valley networks: discharge and runoff production. *Geology* 33, 489–492. <https://doi.org/10.1130/G21333.1>.
- Irwin, R.P., Maxwell, T.A., Howard, A.D., Craddock, R.A., Leverington, D.W., 2002. A large paleolake basin at the head of Ma'adim Vallis. *Mar. Sci.* 296, 2209–2212. <https://doi.org/10.1126/science.1071143>.
- Irwin, R.P., Howard, A.D., Maxwell, T.A., 2004a. Geomorphology of Ma'adim Vallis, Mars, and associated paleolake basins. *J. Geophys. Res.* 109, e12009 <https://doi.org/10.1029/2004JE002287>.
- Irwin, R.P., Craddock, R.A., Howard, A.D., Maxwell, T.A., 2004b. Channels in Martian valley networks: Discharge and runoff production. In: 2004 Conference on Early Mars. Lunar and Planet. Inst, Jackson Hole, Wyo.

- Jaumann, R., Reiss, D., Frei, S., Neukum, G., Scholten, F., Gwinner, K., Roatsch, T., Matz, K.-D., Mertens, V., Hauber, E., Hoffmann, H., Köhler, U., Head, J.W., Hiesinger, H., Carr, M.H., 2005. Interior channels in Martian valleys: constraints on fluvial erosion by measurements of the Mars express high resolution stereo camera. *Geophys. Res. Lett.* 32 (16).
- Kleinhans, M.G., van de Kastelee, H.E., Hauber, E., 2010. Palaeoflow reconstruction from fan Delta morphology on Mars. *Earth Planet. Sci. Lett.* 294 (3–4), 378–392. <https://doi.org/10.1016/j.epsl.2009.11.025>.
- Knighton, D., 1998. *Fluvial Forms and Processes*, 400. Arnold. <https://doi.org/10.4324/9780203784662>.
- Lange, J., 2005. Dynamics of transmission losses in a large arid stream channel. *J. Hydrol.* 306, 112–126.
- Lou, W., Howard, A.D., Craddock, R.A., Oliveira, E.A., Pires, R.S., 2023. Global spatial distribution of Hack's law exponent on Mars consistent early arid climate. *Geophys. Res. Lett.* 50 <https://doi.org/10.1029/2022GL102604> e2022GL102604.
- Luo, W., Stepinski, T.F., 2012. Orientation of valley networks on Mars: the role of impact cratering. *Geophys. Res. Lett.* 39 (24) <https://doi.org/10.1029/2012GL054087>.
- Malin, M.C., Bell, J.F., Cantor, B.A., Caplinger, M.A., Calvin, W.M., Clancy, R.T., Edgett, K.S., Edwards, L., Haberle, R.M., James, P.B., Lee, S.W., Ravine, M.A., Thomas, P.C., Wolff, M.J., 2007. Context camera investigation on board the Mars reconnaissance orbiter. *J. Geophys. Res.* 12, e5 <https://doi.org/10.1029/2006JE002808>.
- Marra, W.A., McLelland, S.J., Parsons, D.R., Murphy, B.J., Hauber, E., Kleinhans, M.G., 2015. Groundwater seepage landscapes from distant and local sources in experiment and on Mars. *Earth. Surf. Dynam.* 3, 389–408. <https://doi.org/10.5194/esurf-3-389-2015>.
- Montgomery, D.R., Dietrich, W.E., 1992. Channel initiation and the problem of landscape scale. *Science.* 255, 826–830. <https://doi.org/10.1126/science.255.5046.826>.
- Mueller, J., 1973. Re-evaluation of the relationship of master streams and drainage basins. *Geol. Soc. Am. Bull.* 84, 3127–3130. [https://doi.org/10.1130/0016-7606\(1972\)83\[3471:ROTROM\]2.0.CO;2](https://doi.org/10.1130/0016-7606(1972)83[3471:ROTROM]2.0.CO;2).
- Neukum, G., Jaumann, R., 2004. HRSC: the High Resolution Stereo Camera of Mars Express. *Mars Express: The Scientific Payload*, 1240, pp. 17–35.
- O'Callaghan, J.F., Mark, D.M., 1984. The extraction of drainage networks from digital elevation data. *Comput. Vision Graphics Image Process.* 28 (3), 323–344. [https://doi.org/10.1016/S0734-189X\(84\)80011-0](https://doi.org/10.1016/S0734-189X(84)80011-0).
- O'Connor, J.E., Baker, V.R., 1992. Magnitudes and implications of peak discharges from glacial Lake Missoula. *GSA Bull.* 104 (3), 267–279. [https://doi.org/10.1130/0016-7606\(1992\)104<0267:MAIOPD>2.3.CO;2](https://doi.org/10.1130/0016-7606(1992)104<0267:MAIOPD>2.3.CO;2).
- Oliveira, E.A., Pires, R.S., Oliveria, R.S., Furtado, V., Hermann, H.J., Andrade Jr., J.S., 2019. A universal approach for drainage basins. *Sci. Rep.* 9, 9845. <https://doi.org/10.1038/s41598-019-46165-0>.
- Ori, G.G., Marinangeli, L., Baliva, A., 2000. Terraces and Gilbert-type deltas in crater lakes in Ismenius Lacus and Memnonia (Mars). *J. Geophys. Res. Planet.* 105 (E7), 17629–17641. <https://doi.org/10.1029/1999JE001219>.
- Orofino, V., Alemanno, G., Di Achille, G., Mancarella, F., 2018. Estimate of the water flow duration in large Martian fluvial systems. *Planet. Space Sci.* 163, 83–96. <https://doi.org/10.1016/j.pss.2018.06.001>.
- Penido, J.C., Fassett, C.I., Som, S.M., 2013. Scaling relationships and concavity of small valley networks on Mars. *Planet. Space Sci.* 75, 105–116. <https://doi.org/10.1016/j.pss.2012.09.009>.
- Phillips, R.J., Zuber, M.T., Solomon, S.C., Golombek, M.P., Jakosky, B.M., Banerdt, W.B., Smith, D.E., Williams, R.M.E., Hynes, B.M., Aharonson, O., Hauck II, S.A., 2001. Ancient geodynamics and global-scale hydrology on Mars. *Science.* 291, 2587–2591. <https://doi.org/10.1126/science.1058701>.
- Ramirez, R.M., Craddock, R.A., Usui, T., 2020. Climate simulations of early Mars with estimated precipitation, runoff, and erosion rates. *J. Geophys. Res. Planets.* 125. <https://doi.org/10.1029/2019JE006160> e2019JE006160.
- Rigon, R., Rodriguez-Iturbe, I., Maritan, A., Tarboton, D.G., Rinaldo, A., 1996. On Hack's law. *Water Resour. Res.* 32, 3367–3374. <https://doi.org/10.1029/96WR02397>.
- Sassolas-Serrayet, T., Cattin, R., Ferry, M., 2018. The shape of watersheds. *Nat. Commun.* 9, 3791. <https://doi.org/10.1038/s41467-018-06210-4>.
- Smith, D.E., Zuber, M.T., Solomon, S.C., et al., 1999. The global topographical of Mars and implications for surface evolution. *Science.* 284, 1495. <https://doi.org/10.1126/science.284.5419.1495>.
- Som, S.M., Montgomery, D.R., Greenberg, H.M., 2009. Scaling relations for large Martian valleys. *J. Geophys. Res. Planet.* 114 (E2). <https://doi.org/10.1029/2008JE003132>.
- Tarboton, D.G., Bras, R.L., Rodriguez-Iturbe, I., 1989. *The Analysis of River Basins and Channel Networks Using Digital Terrain Data*. Tech. Rep, vol. 326. Parsons Lab., Mass. Inst. of Technol, Cambridge.
- Tarboton, D.G., Bras, R.L., Rodriguez-Iturbe, I., 1991. On the extraction of channel networks from digital elevation data. *Hydrol. Process.* 5 (1), 81–100. <https://doi.org/10.1002/hyp.3360050107>.
- Whipple, K.A., Tucker, G.E., 1999. Dynamics of the stream-power river incision model: implications for height limits of mountain ranges, landscape response timescales, and research needs. *J. Geophys. Res. Solid Earth* 104, 17661–17674. <https://doi.org/10.1029/1999JB900120>.
- Willemin, J.H., 2000. Hack's law: sinuosity, convexity, elongation. *Water Resour. Res.* 36, 3365–3374. <https://doi.org/10.1029/2000WR900229>.
- Williams, R.M.E., Phillips, R.J., 2001. Morphometric measurements of Martian valley networks from Mars Orbiter Laser Altimeter (MOLA) data. *J. Geophys. Res.* 106, 23737–23752. <https://doi.org/10.1029/2000JE001409>.
- Yanites, B.J., 2018. The dynamics of channel slope, width, and sediment in actively eroding bedrock river systems. *J. Geophys. Earth Surf.* 123, 1504–1527. <https://doi.org/10.1029/2017JF004405>.